Noncapillary-Wave Structure at the Water-Alkane Interface

Dragoslav M. Mitrinović,[1] Aleksey M. Tikhonov,[1] Ming Li,[1] Zhengqing Huang,[2] and Mark L. Schlossman[1,3,*]

[1]*University of Illinois at Chicago, Department of Physics, 845 West Taylor Street, Chicago, Illinois 60607*

[2]*Brookhaven National Laboratory, National Synchrotron Light Source, Upton, New York 11973*

[3]*University of Illinois at Chicago, Department of Chemistry, 845 West Taylor Street, Chicago, Illinois 60607*

(Received 23 March 2000)

Synchrotron x-ray reflectivity is used to study the interface between bulk water and bulk n-alkanes with carbon numbers 6 through 10, 12, 16, and 22. For all interfaces, except the water-hexane interface, the interfacial width disagrees with the prediction from capillary-wave theory. The variation of interfacial width with carbon number can be described by combining the capillary-wave prediction for the width with a contribution from intrinsic structure. This intrinsic structure is determined by the gyration radius for the shorter alkanes and by the bulk correlation length for the longer alkanes.

PACS numbers: 61.10.Kw, 68.10.–m, 68.35.Ct

Alkanes have been studied extensively as a model for the organization of hydrocarbon chains in soft condensed matter [1]. Ordering at the interface of alkanes with silicon and at the vapor interface of liquid alkanes has been recently reported [2–4]. Optical reflection second harmonic generation has been used to probe the ordering of n-alkanes at the water-alkane interface [5]. Here, we present an x-ray reflectivity study of the interface between bulk liquid water and bulk liquid alkanes. This is an important model system for understanding the interactions between hydrocarbon chains and water, and is therefore of relevance to biological and technological interfacial phenomena.

We previously reported a measurement of the interfacial width between water and hexane [6]. This width was shown to be in agreement with a prediction from capillary-wave theory. Here, we present the extension of those measurements to straight chain alkanes up to 22 carbons long. Significant deviations from the predictions of capillary-wave theory occur for the water interface with these longer alkanes. We present a simple explanation of the variation of interfacial width with alkane chain length.

The measurements presented here are from equilibrium liquid samples in a vapor-tight stainless steel sample cell (discussed elsewhere [6,7]). High purity water was produced by a Barnstead NanoPure system; n-alkanes (99+%) were purchased from Sigma and Fluka. The alkanes were purified by passing them several times through a column of basic alumina [8]. The interfacial tension, measured with a Wilhelmy plate, between these purified alkanes and water was constant to within ± 0.1 dyn/cm as a function of time, where time is measured from the initial formation of the water-alkane interface. Without this purification step, even the highest purity commercially available alkanes showed significant adsorption of impurities to the water-alkane interface as indicated by changes in the interfacial tension of up to 10 to 20 dyn/cm over a period of a few hours.

The interfacial area was 76 mm $\times$ 100 mm (along the beam $\times$ transverse) with x rays penetrating through the upper phase (see Fig. 1). At the chosen x-ray wavelength ($\lambda = 0.825 \pm 0.002$ Å) the absorption lengths for the alkanes and water are approximately 20 and 5.6 mm, respectively. The sample cell is contained in a one-stage cylindrical aluminum thermostat and temperature controlled to ± 0.03 °C. Two thermistors mounted immediately above and below the liquid chamber measure the sample temperature and allow us to determine when the sample cell has thermally equilibrated.

X-ray reflectivity was conducted at beamline X19C at NSLS (Brookhaven National Laboratory, USA) with a liquid surface spectrometer and measurement techniques described elsewhere [7,9]. The kinematics of reflectivity is illustrated in Fig. 1. For specular reflection, the wave vector transfer, $\mathbf{Q} = \mathbf{k}_{\text{scat}} - \mathbf{k}_{\text{in}}$ is only in the z direction, normal to the interface; $Q_x = Q_y = 0$ where x and y are in the plane of the interface, and $Q_z = (4\pi/\lambda)\sin\alpha$.

Two x-ray slits prior to the sample set the incident beam size and reduced the vertical divergence. For the smallest reflection angles the vertical slit gaps were typically 5 to 10 μm, corresponding to a vertical divergence of 20 μrad (horizontal slit gaps were 10 mm, much larger than the horizontal beam size of $\sim$2 mm). A monitor before the sample measured the incident flux. The sample was followed by a slit with a vertical gap of $\sim$2 mm to reduce background scattering and the scintillator detector was preceded by a slit with a vertical gap between 0.4 and 0.6 mm which set the detector resolution.

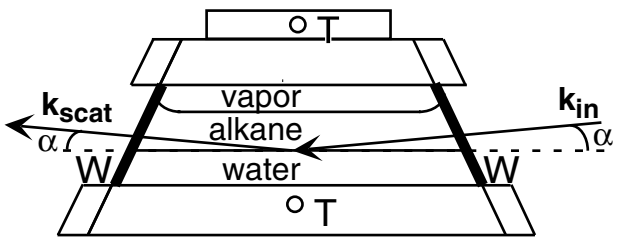

FIG. 1. Cross-sectional view of sample cell: W, Mylar windows; T, thermistors to measure temperature. The kinematics of surface x-ray reflectivity is also indicated: $\mathbf{k}_{\text{in}}$ is the incoming x-ray wave vector, $\mathbf{k}_{\text{scat}}$ is the scattered wave vector, and α is the angle of incidence and reflection.

 0031-9007/00/85(3)/582(4)$15.00 © 2000 The American Physical Society

Figure 2 illustrates x-ray reflectivity measurements for eight different water-alkane interfaces (data for seventeen different samples are shown) [10]. Reflectivity measurements were fit using the error function model for the interfacial profile, with one fitting parameter, σ, which represents interfacial width. This profile describes the variation in electron density as a function of the normal coordinate z through the water-alkane interface, given by

$$\langle \rho(z) \rangle = \frac{1}{2}(\rho_{\mathrm{w}} + \rho_{\mathrm{a1}}) + \frac{1}{2}(\rho_{\mathrm{w}} - \rho_{\mathrm{a1}})\,\mathrm{erf}(z/\sigma\sqrt{2}), \tag{1}$$

where $\langle \rho(z) \rangle$ is the interfacial electron density averaged over the plane of the interface, $\rho_{\mathrm{w,a1}}$ represents the electron densities of bulk water and alkane, and $\mathrm{erf}(z) = (2/\sqrt{\pi}) \int_0^z \exp(-t^2)\,dt$. For this interfacial profile the reflectivity can be written as [11,12]

$$R(Q_z) = R_F(Q_z) e^{-Q_z Q_z^T \sigma^2} \cong \left| \frac{Q_z - Q_z^T}{Q_z + Q_z^T} \right|^2 e^{-Q_z Q_z^T \sigma^2}, \tag{2}$$

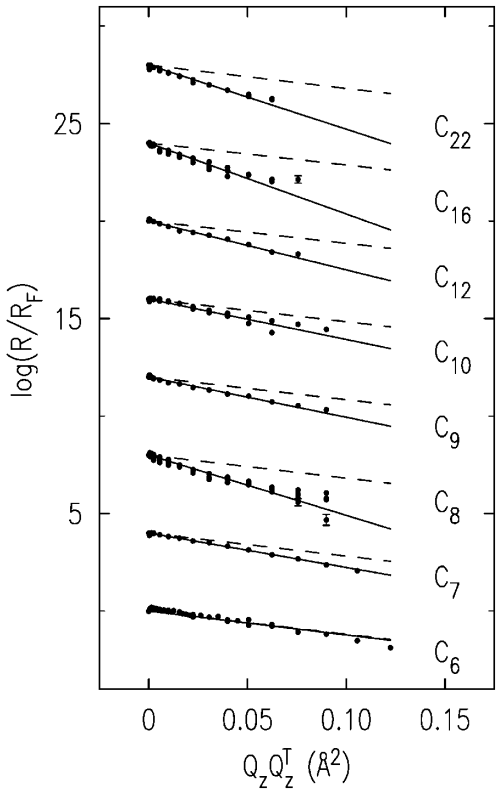

FIG. 2. Logarithm of x-ray reflectivity, normalized to Fresnel reflectivity $R_F(Q_z)$, as a function of $Q_z Q_z^T$, for water-alkane interfaces for eight different n-alkanes. Curves for the different interfaces are offset for clarity. The solid lines are one parameter fits of the measurements to Eq. (2) which determine the interfacial width, σ. Also shown with dashed lines are predicted reflectivity curves for interfaces whose width is determined solely by capillary waves. Note that when presented in this way, reflectivity from Eq. (2) yields a straight line, with a slope of $-\sigma^2$.

where $R_F(Q_z)$, Fresnel reflectivity, is reflectivity calculated for an ideal, zero width, steplike interface, and $Q_z^T \cong (Q_z^2 - Q_c^2)^{1/2}$ is the z component of wave vector transfer with respect to the lower phase. The critical wave vector transfer Q_c is given by the bulk densities as $Q_c = 4[\pi r_e(\rho_{\mathrm{w}} - \rho_{\mathrm{a1}})]^{1/2}$ (where $r_e = e^2/mc^2$), in agreement with our experimental measurements. The data for each interface are separately fit to Eq. (2), and the resulting fit parameters, σ, are listed in Table I. Although more complicated models of the interfacial structure can be proposed, the data are well represented by this simple model (see Fig. 2).

In the spirit of a hybrid model of the interface that describes an intrinsic structural profile roughened by capillary waves, the interfacial width, σ, can be represented as a combination of an intrinsic profile width, σ_0, and a resolution dependent, capillary-wave contribution [13–17]

$$\sigma^2 = \sigma_0^2 + \frac{k_B T}{4\pi^2 \gamma} \iint \frac{d^2\mathbf{q}}{q^2 + \xi_{\parallel}^2} \equiv \sigma_0^2 + \sigma_{\mathrm{cap}}^2, \tag{3}$$

where $k_B T$ is Boltzmann's constant times the temperature, γ is the measured interfacial tension, the correlation length $\xi_{\parallel}$ is given by $\xi_{\parallel}^2 = \gamma/\Delta\rho_m g$ and determines the exponential decay of the interfacial correlations given by the height-height correlation function of interfacial motion [18], $\Delta\rho_m$ is the *mass* density difference of the two phases, and g is the gravitational acceleration. Integration is over in-plane capillary-wave vectors $\mathbf{q}$ corresponding to the range of capillary waves that the measurement probes. After some simplification, the capillary contribution evaluates to $\sigma_{\mathrm{cap}}^2 = k_B T/(2\pi\gamma) \log(q_{\max}/q_{\min})$, where $q_{\max}$ is determined by the cutoff for the capillary waves with the smallest wavelength that the interface can support and $q_{\min} = (2\pi/\lambda)\Delta\beta \sin\alpha$ is determined by the incident angle α and the angular acceptance of the detector $\Delta\beta$ [19].

Using a Wilhelmy plate, we measured the interfacial tension for these different interfaces (see Table I) [8]. The small differences in tension indicate that the contribution to the interfacial width, σ_{cap} [calculated from Eq. (3)], is nearly the same for all these interfaces, $\sigma_{\mathrm{cap}} \cong 3.4$ Å [19]. Calculated predictions for the reflectivity, that would be measured if the only contribution to the interfacial width were from capillary waves, are shown in Fig. 2. It can be seen that the deviation from the capillary-wave contribution is easily measured [20].

In Fig. 3 the interfacial width, σ, is plotted vs carbon number (see also Table I). The dashed line indicates the capillary-wave prediction for the interfacial width and differs significantly from the values of the width σ fit to our data. The other two lines in Fig. 3 are determined by adding in quadrature the capillary-wave contribution and an intrinsic structural contribution to the interfacial width, σ_0, as in Eq. (3). For the line that passes through the lower carbon numbers, the intrinsic width, σ_0, is chosen to be the radius of gyration, R_g, of the alkane. Computer simulations have shown that these short alkanes have an R_g

TABLE I. Measurement temperature, interfacial tension (within 0.5 dyn/cm), calculated capillary-wave interfacial width, measured interfacial width, gyration radius from computer simulation [21], width due to gyration radius and capillary waves combined, and critical wave vector transfer. Error bars on σ_{meas} include both statistical and estimated systematic errors.

Alkane	T (°C)	γ (dyn/cm)	σ_{cap} (Å)	σ_{meas} (Å)	R_g (Å)	$(\sigma_{\text{cap}}^2 + R_g^2)^{1/2}$	Q_c (Å^{-1})
Hexane (C_6)	25	51.3	3.45	3.5 ± 0.2	2.00	3.99	0.01217
Heptane (C_7)	25	51.7	3.44	4.2 ± 0.2	2.28	4.13	0.01169
Octane (C_8)	25	51.8	3.44	5.5 ± 0.2	2.54	4.28	0.01131
Nonane (C_9)	25	52.5	3.41	4.5 ± 0.2	2.80	4.43	0.01099
Decane (C_{10})	25	52.5	3.41	4.6 ± 0.2	3.05	4.58	0.01073
Dodecane (C_{12})	25	53.5	3.38	5.0 ± 0.2	3.54	4.89	0.01032
Hexadecane (C_{16})	25	54.4	3.35	6.0 ± 0.2	4.43	5.55	0.00975
Docosane (C_{22})	44.6	54.4	3.46	5.7 ± 0.2	5.60	6.58	0.00963

expressed as $R_g^2 = c(N)Nl^2$, where l is the carbon-carbon bond length (1.54 Å), N is the number of bonds, and $c(N)$ is a correction factor that varies with bond number [21]. Using the values for R_g from the simulations, the interfacial width is calculated from $\sigma = (R_g^2 + \sigma_{\text{cap}}^2)^{1/2}$, with no adjustable parameters, and plotted in Fig. 3. This line agrees with the lower carbon number data, except for the water-octane interface. The discrepancy with water octane is not understood, however, the data are reproducible.

It is expected that the interfacial structure is independent of chain length for long enough chains. For long chains it has been shown that adsorption of a polymer melt against a hard wall should be governed by a bulk correlation length [22], $\xi_b \sim \rho_b^{-1/2}$, which we write as $\xi_b = c_b(l\rho_b)^{-1/2}$,

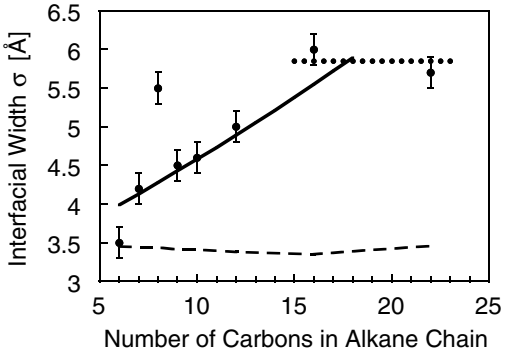

FIG. 3. Interfacial width determined by fitting x-ray reflectivity measurements from the water-alkane interface as a function of alkane carbon number. The error bars are determined from statistical and systematic errors. The dashed line indicates the prediction for the interfacial width from capillary-wave theory (the rise for C_{22} is due to a higher temperature). The solid line through the lower carbon number data is determined, without adjustable parameters, by combining the capillary-wave contribution with an intrinsic interfacial width determined from the gyration radius of the alkane. The horizontal dotted line for the higher carbon numbers is determined, with one adjustable parameter, by combining the capillary-wave contribution with an intrinsic width determined from a bulk correlation length described in the text. The three lines indicate calculations for discrete values of carbon number, but are shown as lines for clarity.

where ρ_b is the bulk monomer number density, c_b is an adjustable parameter of order 1, and l is the carbon-carbon bond length. The dotted line for the higher carbon numbers has been adjusted to pass near the values for C_{16} and C_{22} by choosing $c_b = 1.09$, which yields $\xi_b = 4.8$ Å. An alternative method to estimate the bulk correlation length is from the x-ray diffraction peaks that correspond to intermolecular structure in bulk hydrocarbon liquids. The position of the lowest order peak corresponds to a separation of 4.6 Å which is close to our estimate for ξ_b [23]. The width from the two longer alkanes we measured likely indicates a crossover to this long chain limit.

The measured values of the interfacial widths can be compared to recent predictions from molecular dynamics simulations for water-alkane interfaces: 4.9 ± 1.2 Å for water-hexane [24], 3.2 Å for water-octane [25], 3.3 Å for water-nonane [26], and 3.4 Å for water-decane [27,28]. These simulation results are close to the capillary-wave prediction and in disagreement with our measurements.

We have shown that for short alkanes the gyration radius sets the length scale for intrinsic structure at the interface with water. For longer alkanes the intrinsic structure is set by the bulk correlation length. Except for the simulations just discussed we are not aware of other calculations that can be compared to this result. Helfand and co-workers have predicted $1/n$ corrections in the concentration profile for short chains at the immiscible polymer-polymer interface, but it is not clear if their results are applicable to our measurements [29].

Measurements of the nonlinear susceptibility using optical second harmonic generation suggest that the water-alkane interface may be highly ordered [5]. It is sensible to expect that this molecular order is related to the intrinsic structure that we have measured. For the longer alkane chains our results exclude the possibility that this ordering is due to a perpendicular orientation of the molecules to the interface as seen in studies of surface freezing at the alkane-vapor or alkane-silicon interfaces [2,4]. In that case, oscillations in the reflectivity would be visible [30]. Because of current limitations in the range of Q_z it is not possible to test whether some molecular ordering arises

from alkanes preferentially oriented parallel to the interface. However, models that include molecular layering parallel to the interface require more than one layer to fit our data, and this complex interface is not justified by our current measurements. Orientational order may arise from a preference for chain ends to be at the interface, an effect that becomes more significant for shorter chains. However, since the electron density is lower for methyl groups than for methylene groups in bulk alkanes it seems that just increasing the number of methyl groups at the interface cannot explain our results.

We plan to measure the temperature dependence to help distinguish the two contributions to the interfacial width. Our new facilities at the Advanced Photon Source will allow us to improve the spatial resolution by extending the Q_z range of these measurements. The higher brilliance of the Advanced Photon Source may also allow us to measure off-specular diffuse scattering which will aid in distinguishing interfacial fluctuations from intrinsic structure.

We acknowledge Michael Wilson (Ames Research, NASA) for discussions about computer simulations of water-alkane interfaces and S. V. Pingali for help in purifying the alkanes. This work was supported by the donors of The Petroleum Research Fund administered by the ACS, the UIC Campus Research Board, and the NSF Division of Materials Research. Brookhaven National Laboratory is supported by the U.S. Department of Energy.

*Author to whom correspondence should be addressed. Email address: schloss@uic.edu

[1] D. M. Small, *The Physical Chemistry of Lipids* (Plenum, New York, 1986).
[2] X. Z. Wu *et al.,* Phys. Rev. Lett. **70**, 958 (1993).
[3] B. M. Ocko *et al.,* Phys. Rev. Lett. **72**, 242 (1994).
[4] C. Merkl, T. Pfohl, and H. Riegler, Phys. Rev. Lett. **79**, 4625 (1997).
[5] J. C. Conboy, J. L. Daschbach, and G. L. Richmond, Appl. Phys. A **59**, 623 (1994).
[6] D. M. Mitrinović *et al.,* J. Phys. Chem. **103**, 1779 (1999).
[7] Z. Zhang *et al.,* J. Chem. Phys. **110**, 7421 (1999).
[8] A. Goebel and K. Lunkenheimer, Langmuir **13**, 369 (1997).
[9] M. L. Schlossman *et al.,* Rev. Sci. Instrum. **68**, 4372 (1997).
[10] The path length of the x rays through the upper liquid phase, and therefore the attenuation due to absorption, varies with the reflection angle. This small correction is included in the analysis of the data and is approximately 3% at $Q_z = 0.25$ Å^{-1} (see Ref. [6]).
[11] L. Nevot and P. Croce, Revue Phys. Appl. **15**, 761 (1980).
[12] S. K. Sinha, E. B. Sirota, S. Garoff, and H. B. Stanley, Phys. Rev. B **38**, 2297 (1988).
[13] J. D. Weeks, J. Chem. Phys. **67**, 3106 (1977).
[14] A. Braslau *et al.,* Phys. Rev. Lett. **54**, 114 (1985).
[15] A. Braslau *et al.,* Phys. Rev. A **38**, 2457 (1988).
[16] D. K. Schwartz *et al.,* Phys. Rev. A **41**, 5687 (1990).
[17] M. L. Schlossman, in *Encyclopedia of Applied Physics,* edited by G. L. Trigg (VCH Publishers, New York, 1997), p. 311.
[18] M. P. Gelfand and M. E. Fisher, Physica (Amsterdam) **166A**, 1 (1990).
[19] Integration is over a circular region in reciprocal space, of radius $q_{\max} = (2\pi/5)$ Å^{-1}, with a cutout in the center. The cutout is determined by the known resolution of the spectrometer, so that x rays scattered by capillary waves with wave vectors **q** outside of the cutout region (thus, within the integration region) are deflected outside the angular acceptance of a detector centered on the position for specular reflection. For the values of σ_{cap} in Table I, α is chosen to be 0.94° (corresponding to $Q_z = 0.25$ Å^{-1}) and $\Delta\beta = 0.6/676$ rad. We chose 5 Å, in the expression for $q_{\max}$ to correspond to the approximate chain-chain distance. However, the value of σ_{cap} is insensitive to the exact choice of $q_{\max}$. For example, varying $q_{\max}$ by a factor of 2 results in a change of only 3% to σ_{cap}.
[20] Note that adjusting $q_{\max}$ to yield values of σ_{cap} in agreement with our measured values of σ would require using nonphysically large values of $q_{\max}$.
[21] G. Avitabile and A. Tuzi, J. Polymer Sci. **21**, 2379 (1983).
[22] E. Eisenriegler, J. Chem. Phys. **79**, 1052 (1983).
[23] A. Habenschuss and A. H. Narten, J. Chem. Phys. **91**, 4299 (1989).
[24] I. L. Carpenter and W. J. Hehre, J. Phys. Chem. **94**, 531 (1990).
[25] Y. Zhang *et al.,* J. Chem. Phys. **103**, 10 252 (1995).
[26] D. Michael and I. Benjamin, J. Phys. Chem. **99**, 1530 (1995).
[27] A. R. v. Buuren, S.-J. Marrink, and H. J. C. Berendsen, J. Phys. Chem. **97**, 9206 (1993).
[28] The simulation cells have interfacial areas of typically (3 nm)^2 and, therefore, contain only a small part of the capillary wave spectrum probed by our reflectivity measurements. Using Eq. (3) we calculated the additional contribution to the width due to extending the simulation cell size to the longest capillary wavelengths measured by our experiment. To calculate this contribution we set $q_{\max}$ to $\pi/30$ Å^{-1}, corresponding to the longest capillary wavelength that the simulation cell can support and we use $q_{\min}$ appropriate for our spectrometer resolution.
[29] E. Helfand, S. M. Bhattacharjee, and G. H. Fredrickson, J. Chem. Phys. **91**, 7200 (1989).
[30] A. M. Tikhonov *et al.,* J. Phys. Chem. (to be published).